Inhibition or Deletion of Soluble Epoxide Hydrolase Prevents Hyperglycemia, Promotes Insulin Secretion, and Reduces Islet Apoptosis

Pengcheng Luo, Hsin-Hsin Chang, Yiqiang Zhou, Shali Zhang, Sung Hee Hwang, Christophe Morisseau, Cong-Yi Wang, Edward W. Inscho, Bruce D. Hammock, and Mong-Heng Wang

Department of Physiology (P.L., H.-H.C., Y.Z., S.Z., E.W.I., M.-H.W.) and Center for Biotechnology and Genomic Medicine, Department of Pathology (C.-Y.W.), Medical College of Georgia, Augusta, Georgia; Department of Nephrology, Renmin Hospital of Wuhan University, Hubei Province, China (P.L.); and Department of Entomology and Cancer Center, University of California, Davis, California (S.H.H., C.M., B.D.H.)

ABSTRACT

Soluble epoxide hydrolase (sEH) is an enzyme involved in the metabolism of endogenous inflammatory and antiapoptotic mediators. However, the roles of sEH in diabetes and the pancreas are unknown. Our aims were to determine whether sEH is involved in the regulation of hyperglycemia in diabetic mice and to investigate the reasons for the regulation of insulin secretion by sEH deletion or inhibition in islets. We used two separate approaches, targeted disruption of $Ephx2$ gene [sEH knockout (KO)] and a selective inhibitor of sEH [$trans$-4-[4-(3-adamantan-1-ylureido)-cyclohexyloxy]-benzoic acid (t-AUCB)], to assess the role of sEH in glucose and insulin homeostasis in streptozotocin (STZ) mice. We also examined the effects of sEH KO or t-AUCB on glucose-stimulated insulin secretion (GSIS) and intracellular calcium levels in islets. Hyperglycemia in STZ mice was prevented by both sEH KO and t-AUCB. In addition, STZ mice with sEH KO had improved glucose tolerance. More important, when insulin levels were assessed by hyperglycemic clamp study, sEH KO was found to promote insulin secretion. In addition, sEH KO and t-AUCB treatment augmented islet GSIS. Islets with sEH KO had a greater intracellular calcium influx when challenged with high glucose or KCl in the presence of diazoxide. Moreover, sEH KO reduced islet cell apoptosis in STZ mice. These results show not only that sEH KO and its inhibition prevent hyperglycemia in diabetes, but also that sEH KO enhances islet GSIS through the amplifying pathway and decreases islet cell apoptosis in diabetes.

The prevalence of diabetes continues to increase. It is estimated that 225 million people are affected worldwide (Mazzone, 2009). Moreover, the diabetic population is subject to a high incidence of cardiovascular and renal diseases (Breyer et al., 2005; Mazzone, 2009). Diabetes is characterized by hyperglycemia related to abnormalities in the function of pancreatic β cells. Because β-cell destruction and dysfunction are the central events in the development and progression of diabetes, the prevention of β-cell destruction and the improvement of β-cell function could be important strategies for controlling the advance of diabetes (Kahn et al., 2006; Donath et al., 2008).

In pancreatic β cells, glucose stimulates insulin secretion by activating the triggering and amplifying pathways (Henquin, 2000). In the triggering pathway, products of glucose metabolism enter the mitochondrial respiratory chain, which uses them to generate ATP. Increased ATP levels close the K_{ATP}-sensitive channels, followed by membrane depolarization and opening of the voltage-sensitive Ca^{2+} channels, which in turn increase intracellular Ca^{2+} concentration and

ABBREVIATIONS: UCP2, uncoupling protein 2; GSIS, glucose-stimulated insulin secretion; $[Ca^{2+}]_i$, intracellular calcium concentration; sEH, soluble epoxide hydrolase; EET, epoxyeicosatrienoic acid; P450, cytochrome P450; DHET, dihydroxyeicosatrienoic acid; t-AUCB, $trans$-4-[4-(3-adamantan-1-ylureido)-cyclohexyloxy]-benzoic acid; KO, knockout; STZ, streptozotocin; bp, base pair; ELISA, enzyme-linked immunosorbent assay; IGTT, intraperitoneal glucose tolerance test; AUC, area under the curve; DMEM, Dulbecco's modified Eagle's medium; TUNEL, terminal deoxynucleotidyl transferase dUTP nick-end labeling.

promote insulin secretion. In this pathway, uncoupling protein 2 (UCP2) acts as a negative regulator of glucose-stimulated insulin secretion (GSIS) by decreasing the production of ATP (Krauss et al., 2003). The amplifying pathway augments insulin release independently from its action on K_{ATP}-sensitive channels. The amplifying pathway can be studied by clamping intracellular calcium concentration ($[Ca^{2+}]_i$) with high KCl in the presence of diazoxide, which holds K_{ATP}-sensitive channels open (Gembal et al., 1992).

It has been recognized that soluble epoxide hydrolase (sEH), an enzyme, adds water to epoxide substrates, forming their corresponding 1,2-diol products. Extensive evidence has shown that the protective effects of sEH inhibition are consequences of its ability to metabolize epoxyeicosatrienoic acids (EETs) (Chiamvimonvat et al., 2007). EETs, cytochrome P450 (P450)-derived eicosanoids, have important biological properties in the kidneys and cardiovascular system (Roman, 2002; Imig, 2006). In the presence of NADPH and oxygen, arachidonic acid is metabolized by P450 epoxygenases into four EETs: 5,6-EET, 8,9-EET, 11,12-EET, and 14,15-EET. EETs are metabolized by sEH to the corresponding dihydroxyeicosatrienoic acids (DHETs) (Roman, 2002). In general, DHETs are much less biologically active than are EETs (Imig, 2005; Deng et al., 2010). Therefore, inhibition of sEH activity has been used as a means of studying the biological functions of EETs (Imig, 2005, 2006).

Although it is well established that sEH inhibition has beneficial effects in cardiovascular and renal diseases (Imig, 2005; Chiamvimonvat et al., 2007), the role of sEH in diabetes is still unknown. Several selective sEH inhibitors have been developed for long-term in vivo studies (Liu et al., 2009). *trans*-4-[4-(3-Adamantan-1-ylureido)-cyclohexyloxy]-benzoic acid (*t*-AUCB) is a newly developed potent sEH inhibitor (Liu et al., 2009) that has greater metabolic stability in vivo than do many sEH inhibitors (Liu et al., 2009). In the present study, we investigated whether *t*-AUCB and sEH knockout (KO) [*Ephx2*(−/−)] have any effects on the control of blood glucose homeostasis in streptozotocin (STZ)-treated mice. To control for any hemodynamic alternations, we also examined the role of sEH in β-cell function using isolated islets. To investigate whether sEH is involved in the prevention of β-cell loss, we also examined the effects of sEH KO on islet cell apoptosis in diabetes.

Materials and Methods

Experimental Animal and Genotypic Analysis. *Ephx2*(−/−) (B6.129X-*Ephx2*[tm1gonz]/J) mice were obtained from The Jackson Laboratory (Bar Harbor, ME). These mice were backcrossed with C57BL/6J mice for five generations to produce heterozygous *Ephx2*(+/−) offspring. The resulting *Ephx2*(+/−) offspring were intercrossed to generate *Ephx2*(+/+) and *Ephx2*(−/−) mice.

We obtained tail snips from litters at weaning (approximately 3 weeks of age). The DNA from tail snips was used to identify murine genotype by polymerase chain reaction. Routine genotyping of *Ephx2*(+/+), *Ephx2*(+/−), and *Ephx2*(−/−) mice was done using the following primers: F1, 5′-CTTGGCAGGGTTTCTAGTC-CTTAG-3′; R1, 5′-CACGCTGGCATTTTAACACCAG-3′; F2, 5′-CGCTTCCTCGTGCTTTACGGTATC-3′; and R2, GTCAAGGTC-GAACGCGGCTACAC-3′. Primer F1/R1 predicts a 510-base pair (bp) amplicon for the wild-type allele. For the *Ephx2*-null allele, primer F2/R2 predicts a 160-bp product of a neomycin-resistance sequence as described previously (Sinal et al., 2000). These primers

were designed by Lasergene 7 software (DNAstar, Madison, WI). The genotypic analysis was examined using 3% Nusieve GTG agarose gel (Lonza Rockland, Inc., Rockland, ME). All the animal protocols were approved by the Institutional Animal Care and Use Committee and were in accord with the requirements stated in the *Guide for the Care and Use of Laboratory Animals* (Institute of Laboratory Animal Resources, 1996).

Western Blot Analysis. Expression of sEH, UCP2, and β-actin was analyzed by homogenization of tissues or cells. Samples from *Ephx2*(+/+) and *Ephx2*(−/−) mice, as well as NIT-1 cells, were separated by electrophoresis for 3 h. The proteins were transferred to an enhanced chemiluminescence membrane in a transfer buffer. The membranes were blocked for 90 min with 5% nonfat dry milk in Tris-buffered saline. The membranes were incubated with antibody against human sEH (1:1000), against mouse UCP2 (1:500; Alpha Diagnostic, San Antonio, TX), or against β-actin (1:5000; Sigma-Aldrich, St. Louis, MO). The membranes were incubated with secondary antibody for sEH, UCP2, or β-actin. Chemiluminescent detection using enhanced chemiluminescence reagent from GE Healthcare (Little Chalfont, Buckinghamshire, UK) was done on X-ray film. In addition, quantification of sEH levels in mouse islets was done with the Odyssey infrared imaging system (LI-COR Biosciences, Lincoln, NE) and analyzed with National Institutes of Health ImageJ software (http://rsb.info.nih.gov/ij/).

STZ-Induced Diabetes and the Treatment of *t*-AUCB. Diabetes was induced in *Ephx2*(+/+) and *Ephx2*(−/−) mice by injection of STZ as described previously (Yoon et al., 2001). We treated 6-week-old male *Epxh2*(+/+) mice with STZ (50 mg/kg/day for 3 days, i.p.), STZ plus *t*-AUCB (10 mg/l in drinking water), or vehicle. We also treated age-matched *Ephx2*(−/−) mice with the same dose of STZ or vehicle.

Blood Glucose, Plasma Insulin, and Plasma Glucagon. Blood glucose concentrations were measured with a glucometer (Accu-Check blood glucose monitor system; Roche Diagnostics, Indianapolis, IN). Plasma insulin concentrations were measured using mouse insulin as a standard [rat insulin enzyme-linked immunosorbent assay (ELISA) kit; Crystal Chemical, Chicago, IL]. Plasma glucagon concentrations were measured using a glucagon ELISA kit (Cosmo Bio, Tokyo, Japan).

Hyperglycemic Clamp and Glucose Tolerance Studies. Hyperglycemic clamp study was done using continuous infusion of glucose from the jugular vein in a modified version of a previously published method (Danial et al., 2008). Male *Ephx2*(−/−) and *Ephx2*(+/+) mice aged 12 to 18 weeks were cannulated with tubing (o.d. 0.64 mm; Silastic, Midland, MI) into the right internal jugular vein for continuous infusion of glucose. After 2 to 3 days of recovery from surgery, clamp analysis was done on 6-h fasted and conscious mice. Variable infusion of a 20% glucose solution was started at time 0 and periodically adjusted to sequentially clamp plasma glucose concentrations at approximately 450 mg/dl. Blood samples were collected from mouse tails at 5- to 10-min intervals for 120 min for use in the measurement of plasma insulin by an ELISA kit (LINCO Research, St. Charles, MO). Intraperitoneal glucose tolerance tests (IGTTs) were performed on 12- to 16-week-old mice. STZ mice were fasted for 6 h and given intraperitoneal injections of glucose (1 g/kg b.wt.). Blood glucose concentrations were determined with a glucometer at 0, 10, 30, 60, and 120 min after glucose administration (Uysal et al., 1997). Plasma insulin concentrations were determined by an ELISA kit at 0, 30, 60, and 120 min after glucose administration. The values of area under the curve for blood glucose ($AUC_{glucose}$) and insulin ($AUC_{insulin}$) in IGTT were determined by GraphPad Software, Inc. (San Diego, CA). Insulin tolerance tests were performed similarly by injecting human insulin (1 U/kg b.wt.). Glucose concentrations were measured at 0, 10, 30, and 60 min after insulin administration.

Pancreatic Islet Isolation, Insulin Secretion, Islet ATP Concentrations, and Islet Cell Apoptosis. Pancreatic islets were isolated by a modified collagenase digestion method as described pre-

viously (Zhang et al., 2001; Oshima et al., 2006). Anesthetized *Ephx2*(−/−) and *Ephx2*(+/+) mice were sacrificed by cervical dislocation. The common duct was clamped at its entrance to the duodenum and cannulated under a dissecting microscope. Pancreatic inflation was accomplished via the bile duct with 2.0 to 2.5 ml of 0.5 mg/ml collagenase XI (Roche Diagnostics) dissolved in Hanks' buffer supplemented with 1 mM $MgCl_2$ and 10 mM HEPES. The distended pancreases were removed and incubated with type XI collagenase (Roche Diagnostics) in glass vials for approximately 17 min at 37°C. During the incubation, we manually agitated the glass vials containing pancreases to achieve tissue disintegration. The islets were hand-picked three to four times under a dissecting microscope; we estimated that we obtained approximately 80 to 100 islets/mouse. We then cultured islets overnight in Dulbecco's modified Eagle's medium (DMEM) containing 8.3 mM glucose and supplemented with 1% penicillin-streptomycin, 7.5% fetal bovine serum, and 10 mM HEPES at 37°C. Islets were pooled and washed three times with Krebs' buffer (119 mM NaCl, 4.6 mM KCl, 1 mM $MgSO_4$, 0.15 mM Na_2HPO_4, 0.4 mM KH_2PO_4, 25 mM $NaHCO_3$, 2 mM $CaCl_2$, 20 mM HEPES at pH 7.4 and 0.05%, w/v, bovine serum albumin). The islets (5 islets/sample) were then incubated in Krebs' buffer containing 3 mM glucose for 1 h at 37°C and pelleted (800*g* for 5 min), after which their medium was aspirated and replaced for 1 h with 1.0 ml of Krebs' solution containing different concentrations of glucose or 30 mM KCl plus 250 μM diazoxide plus 3 mM glucose. KCl solutions were prepared by equimolar substitution of NaCl to maintain iso-osmolarity. Five parallel repeats were done for each condition. Islet ATP concentrations were determined by a luciferase-based assay on 50 islets/tube as described previously (Krauss et al., 2003). For in vitro sEH inhibition experiments, *Ephx2*(+/+) islets were treated in the same manner except that DMEM and Krebs' buffer containing 100 μM *t*-AUCB dissolved in dimethyl sulfoxide were used. All pellets were solubilized to assess intracellular insulin content. The supernatant and pellets were collected and assayed for insulin using an ELISA kit (LINCO Research). Insulin release data were determined by the ratio of insulin levels in supernatant to insulin levels in pellets. To determine islet apoptosis, mouse pancreases isolated from *Ephx2*(−/−) and *Ephx2*(+/+) mice given different treatments were fixed, sectioned, and terminal deoxynucleotidyl transferase dUTP nick-end labeling (TUNEL)-stained. The TUNEL assay was done using the ApopTag Plus Peroxidase In Situ Apoptosis Detection Kit (Millipore Corporation, Billerica, MA) according to the manufacturer's instructions. Apoptosis was scored as the average number of TUNEL-positive cells per 100 islet cells. The data were expressed as the relative fold change of TUNEL-positive cells per 100 islet cells in the STZ-*Ephx2*(+/+) group compared with the STZ-*Ephx2*(−/−) group (Dai et al., 2009).

[Ca²⁺]$_i$ Measurement in Islet Cells. Fluorescence experiments were performed using monochromator-based fluorescence spectrophotometry (Photon Technology International, London, ON, Canada) as described previously (Inscho et al., 1999). Excitation wavelengths were set at 340 and 380 nm; emitted light was collected at 510 ± 20 nm. Fluorescence intensity was collected at 10 data points/s. These data were analyzed using FeliX software (Photon Technology International).

Islets were dissociated into single cells by incubation in trypsin at 37°C for 10 min and then washed twice before being allowed to attach to glass coverslips. Cells were incubated overnight in RPMI 1640 medium with 10% fetal bovine serum and 1% penicillin-streptomycin. Cells were transferred to a fura-2 loading solution containing 5 μM fura-2 acetoxymethyl ester (fura-2-AM; Invitrogen, Carlsbad, CA) in serum-free DMEM for 30 to 45 min at 37°C. Coverslips of fura-2-loaded cells were mounted in a perfusion chamber (Warner Instruments, Hamden, CT) and affixed to the stage of an Olympus (Tokyo, Japan) IX50 inverted light microscope. The cells were continuously superfused (1.4 ml/min; 25°C) with normal Ca²⁺ solution (120 mM NaCl, 5 mM KCl, 25 mM $NaHCO_3$, 2.5 mM $CaCl_2$, 1.1 mM $MgCl_2$, and 25 mM HEPES, titrated to pH 7.4) containing 3 mM glucose and then challenged with 25 mM glucose or 30 mM KCl plus 250 μM diazoxide plus 3 mM glucose. High K⁺ solutions were prepared by equimolar substitutions of KCl for NaCl. Fluorescence data were collected with background subtraction.

Statistical Analysis. All the values are expressed as mean ± S.E. All the data were analyzed by SPSS computer software (SPSS Inc., Chicago, IL). We used one-way analysis of variance and Student-Newman-Keuls tests for multiple comparisons or independent Student's *t* test for unpaired groups. Statistical significance was set at $P < 0.05$ or 0.01.

Results

Genotyping for *Ephx2*(−/−), *Ephx2*(+/−), and *Ephx2*(+/+) Mice. Heterozygous *Ephx2*(+/−) mice were interbred to generate homozygous *Ephx2*(−/−) mice and their littermate controls, *Ephx2* (+/+)mice. The genotypes of *Ephx2*(−/−), *Ephx2*(+/−), and *Ephx2*(+/+) mice are shown in Fig. 1A. To confirm that sEH protein is deleted in
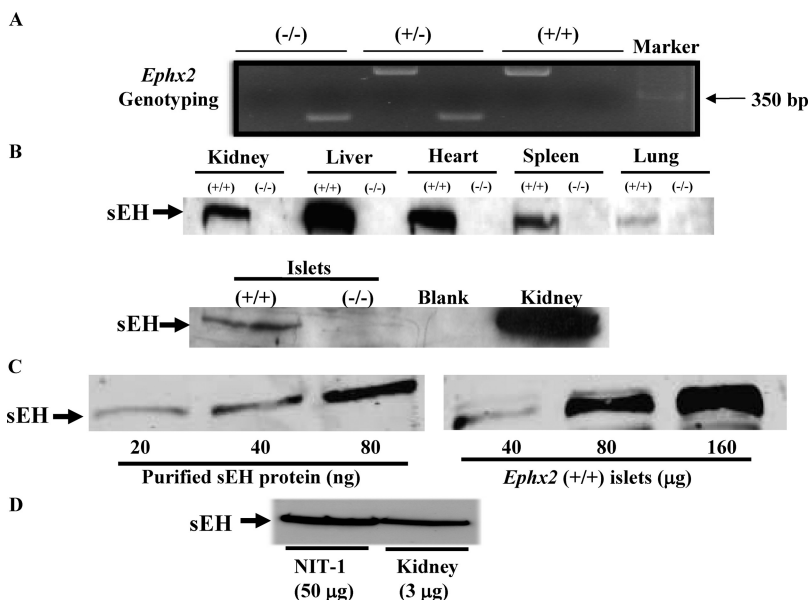

Fig. 1. Genotyping and sEH tissue distribution. A, representative genotypic analysis of *Ephx2*(−/−) mice. Genomic DNA was isolated from mouse tails. The polymerase chain reaction products of *Ephx2*(−/−), *Ephx2*(+/−), and *Ephx2*(+/+) mice showed, respectively, a 160-bp band, 160- and 510-bp bands, and a 510-bp band. B, tissue distribution of sEH protein from *Ephx2*(+/+) and *Ephx2*(−/−) mice. Western blot analysis showed the expression of sEH protein in the kidney, liver, heart, spleen, lung, and islets of *Ephx2*(+/+) mice. In contrast, sEH protein expression was absent from the tissues in *Ephx2*(−/−) mice. Based on protein standards (Bio-Rad Laboratories, Hercules, CA), the size of sEH protein is approximately 62 kDa. C, different concentrations of recombinant murine sEH (20–80 ng) and protein (40–160 μg) of *Ephx2*(+/+) islets for Western blot analysis. D, Western blot of sEH in NIT-1 cells (50 μg of protein) and mouse kidneys (3 μg of protein).

$Ephx2(-/-)$ mice, Western blot analysis was done on tissues isolated from $Ephx2(+/+)$ and $Ephx2(-/-)$ mice. As shown in Fig. 1B, sEH protein was expressed in different tissues of $Ephx2(+/+)$ mice but was absent in $Ephx2(-/-)$ mice. In addition, we estimated that the concentration of sEH in mouse islets is approximately 0.93 ng/μg protein (Fig. 1C). To determine whether sEH is expressed in β cells, we did Western blot analysis of sEH in NIT-1 cells (nonobese diabetic mouse–derived β-cell line). We found that sEH is expressed in these cells (Fig. 1D), suggesting that sEH is expressed in β cells.

sEH KO and Inhibition Prevent Hyperglycemia in STZ-Diabetic Mice. To investigate the effect of sEH KO on glucose homeostasis in diabetes, we induced diabetes in $Ephx2(-/-)$ and $Ephx2(+/+)$ mice by injecting them with a low dose of STZ (50 mg/kg/day of STZ for 3 days, i.p.). To determine whether sEH inhibition has effects similar to those of sEH KO, we simultaneously treated $Ephx2(+/+)$ mice with STZ and t-AUCB. $Ephx2(+/+)$ mice treated with STZ had elevated blood glucose. t-AUCB treatment prevented hyperglycemia in $Ephx2(+/+)$ mice treated with STZ (Fig. 2). Blood glucose levels in STZ-treated $Ephx2(-/-)$ mice were only slightly elevated (Fig. 2). In addition, we found no difference in the average blood glucose values of $Ephx2(+/+)$ and $Ephx2(-/-)$ mice injected with vehicle. These intriguing results provide convincing evidence that sEH deletion and its inhibition prevent hyperglycemia in STZ-induced diabetes.

sEH KO Causes Higher Plasma Insulin Levels. To determine the effects of sEH KO on glucose and insulin homeostasis, we did IGTT on STZ-$Ephx2(-/-)$ and STZ-$Ephx2(+/+)$ mice. $AUC_{glucose}$ in STZ-$Ephx2(-/-)$ mice was significantly lower than that in STZ-$Ephx2(+/+)$ mice

(48,360 ± 2468 versus 63,855 ± 3254 mg/dl × 120 min; $n = 4$; $P < 0.05$) (Fig. 3A). These results show that STZ-$Ephx2(-/-)$ mice have significantly greater glucose tolerance than do STZ-$Ephx2(+/+)$ mice. In contrast, $AUC_{insulin}$ in STZ-$Ephx2(-/-)$ mice was significantly higher than that in STZ-$Ephx2(+/+)$ mice (45 ± 2.6 versus 30 ± 4.3 ng/ml × 120 min; $n = 4$; $P < 0.05$). It appears that the reason for increasing $AUC_{insulin}$ in STZ-$Ephx2(-/-)$ mice is because STZ-$Ephx2(-/-)$ mice have higher basal insulin levels than STZ-$Ephx2(+/+)$ mice (Fig. 3B).

To determine the effect of sEH on in vivo insulin secretion, we used hyperglycemic clamp study to assess insulin secretion in $Ephx2(-/-)$ and $Ephx2(+/+)$ mice (Fig. 4A). Fasting $Ephx2(-/-)$ and $Ephx2(+/+)$ mice were infused with intravenous glucose as needed to maintain blood glucose levels at ~450 mg/dl in both groups. $Ephx2(-/-)$ mice required a considerably higher glucose infusion rate than did $Ephx2(+/+)$ mice to maintain this blood glucose concentration (Fig. 4B). Moreover, the insulin secretion response in $Ephx2(-/-)$ mice during hyperglycemia was significantly higher than that in $Ephx2(+/+)$ mice (Fig. 4C), providing important evidence that sEH KO increases GSIS in vivo. Insulin tolerance tests showed that insulin sensitivity was equal in $Ephx2(+/+)$ and $Ephx2(-/-)$ mice (Fig. 5A). To evaluate whether glucagon is involved in the regulation of blood glucose concentrations in $Ephx2(-/-)$ mice, we determined fed and fasted plasma glucagon levels in $Ephx2(-/-)$ and $Ephx2(+/+)$ mice, finding they were similar (Fig. 5B).

sEH KO and Inhibition Increase Insulin Secretion in Islets. Because both $Ephx2$ gene deletion and pharmacological inhibitors suppress sEH activity throughout the body, it is hard to determine whether the effects of sEH deletion and inhibition are pancreas-specific or reflect whole-body actions. In addition, hemodynamic effects resulting from sEH inhibition or deficiency may cause altered insulin secretion. To evaluate the direct effects of sEH KO on insulin secretion, and to determine whether this enhanced insulin secretion is also manifested in vitro, islets harvested from $Ephx2(+/+)$ and $Ephx2(-/-)$ mice were challenged with 3 mM glucose, 25 mM glucose, or 30 mM KCl plus 250 μM diazoxide plus 3 mM glucose. $Ephx2(-/-)$ and $Ephx2(+/+)$ islets incubated with 3 mM glucose secreted similar amounts of insulin. However, when islets were challenged with 25 mM glucose, $Ephx2(-/-)$ islets secreted significantly greater amounts of insulin than did $Ephx2(+/+)$ islets. Insulin secretion stimulated by KCl plus diazoxide plus 3 mM glucose was significantly higher in $Ephx2(-/-)$ islets than in
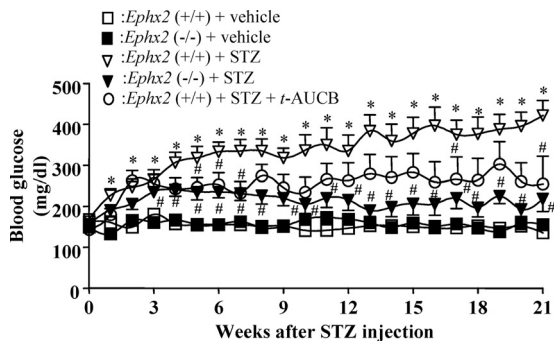
Fig. 2. Effects of sEH KO or inhibition on blood glucose levels in STZ mice. Weekly fasting blood glucose levels of $Ephx2(+/+)$ + STZ ($n = 10$), $Ephx2(-/-)$ + STZ ($n = 11$), $Ephx2(+/+)$ + STZ + t-AUCB (10 mg/l in drinking water; $n = 5$), $Ephx2(+/+)$ + vehicle ($n = 5$), and $Ephx2(-/-)$ + vehicle ($n = 5$) after STZ treatment. *, $P < 0.05$ versus $Ephx2(+/+)$ + vehicle; #, $P < 0.05$ versus $Ephx2(+/+)$ + STZ.
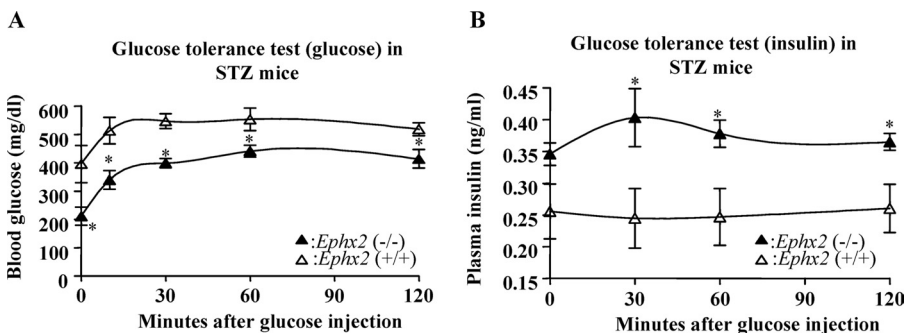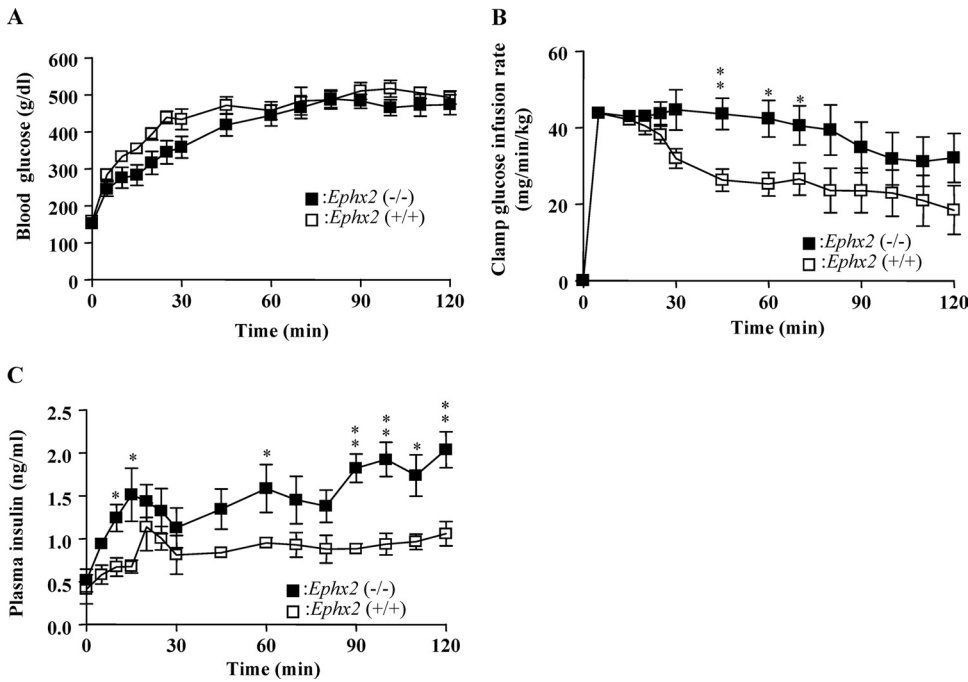
Fig. 3. Glucose and insulin homeostasis in $Ephx2(+/+)$ and $Ephx2(-/-)$ mice treated with STZ. IGTT in STZ-induced diabetic mice. After a 6-h fast, mice received i.p. injections of 1 g/kg glucose (time = 0). Blood glucose (A) and insulin (B) were measured before and at varying time points after glucose administration. The following mice were used: STZ-$Ephx2(+/+)$ mice ($n = 4$) and STZ-$Ephx2(-/-)$ mice ($n = 4$). *, $P < 0.05$ versus STZ-$Ephx2(+/+)$.

Fig. 4. Hyperglycemic clamp study in $Ephx2(-/-)$ and $Ephx2(+/+)$ mice. Blood glucose levels ($n = 6$) (A), glucose infusion rate ($n = 5$) (B), and plasma insulin levels ($n = 4$) (C) before and during hyperglycemic clamp. ∗, $P < 0.05$; ∗∗, $P < 0.01$ versus $Ephx2(+/+)$.
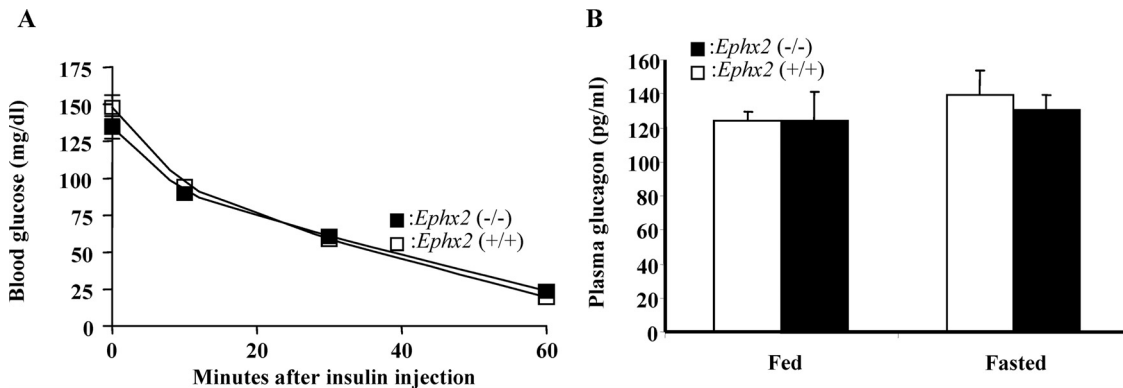

Fig. 5. A, Intraperitoneal insulin tolerance tests in $Ephx2(+/+)$ and $Ephx2(-/-)$ mice. After 6-h fast, mice ($n = 4$) from each group were injected with 1 U/kg human insulin i.p. (time = 0). Blood glucose concentrations were measured before and at 10, 30, and 60 min after insulin administration. B, fed ($n = 5$) and fasted ($n = 4$) glucagon levels in $Ephx2(+/+)$ and $Ephx2(-/-)$ mice. Glucagon levels in $Ephx2(-/-)$ mice were indistinguishable from those of their littermate control, $Ephx2(+/+)$ mice.

$Ephx2(+/+)$ islets (Fig. 6A). We also incubated $Ephx2(+/+)$ islets with or without t-AUCB (100 μM) and challenged them with 25 mM glucose. Under these conditions, $Ephx2(+/+)$ islets incubated with t-AUCB secreted significantly higher amounts of insulin than did vehicle-treated islets (Fig. 6B). Likewise, insulin secretion by $Ephx2(+/+)$ islets incubated with t-AUCB and stimulated with KCl plus diazoxide plus 3 mM glucose was significantly higher than that in the absence of t-AUCB incubation (Fig. 6B). To determine whether sEH KO has any effect on ATP levels, $Ephx2(-/-)$ and $Ephx2(+/+)$ islets were incubated with varying concentrations of glucose. sEH KO did not affect ATP concentrations in islets incubated with either 3 or 25 mM glucose (Fig. 6C). To assess whether sEH KO has any effect on UCP2, we determined the expression levels of UCP2 by Western blot analysis in $Ephx2(-/-)$ and $Ephx2(+/+)$ islets, finding that sEH KO did not affect expression levels of UCP2 (Fig. 6D).

sEH KO Increases $[Ca^{2+}]_i$ Response to High Glucose and KCl Plus Diazoxide. To determine whether sEH KO

affects $[Ca^{2+}]_i$ in response to different stimulators, we monitored changes in $[Ca^{2+}]_i$ in $Ephx2(-/-)$ and $Ephx2(+/+)$ islet cells exposed to 3 mM glucose, 25 mM glucose, or 30 mM KCl plus 250 μM diazoxide plus 3 mM glucose. Basal $[Ca^{2+}]_i$ levels were similar at 3 mM glucose in $Ephx2(-/-)$ and $Ephx2(+/+)$ islet cells, suggesting that sEH KO does not affect the basic control mechanism of Ca^{2+} handling. Compared with 3 mM glucose, $[Ca^{2+}]_i$ increased rapidly in response to 25 mM glucose in both $Ephx2(-/-)$ and $Ephx2(+/+)$ islet cells. However, $Ephx2(-/-)$ cells exhibited higher $[Ca^{2+}]_i$ levels than did $Ephx2(+/+)$ cells (Figs. 7, A and B); these results paralleled those for insulin secretion in islets (Fig. 6A). Likewise, the effects of KCl plus diazoxide plus 3 mM glucose on $[Ca^{2+}]_i$ were significantly greater in $Ephx2(-/-)$ cells than in $Ephx2(+/+)$ cells (Fig. 7).

sEH KO Reduces Islet Cell Apoptosis in STZ Mice. It is well established that immune cell-secreted proinflammatory cytokines are important in the pathogenesis of STZ-induced diabetes (Müller et al., 2002; Fukuda et al., 2008). These proinflammatory cytokines promote islet cell
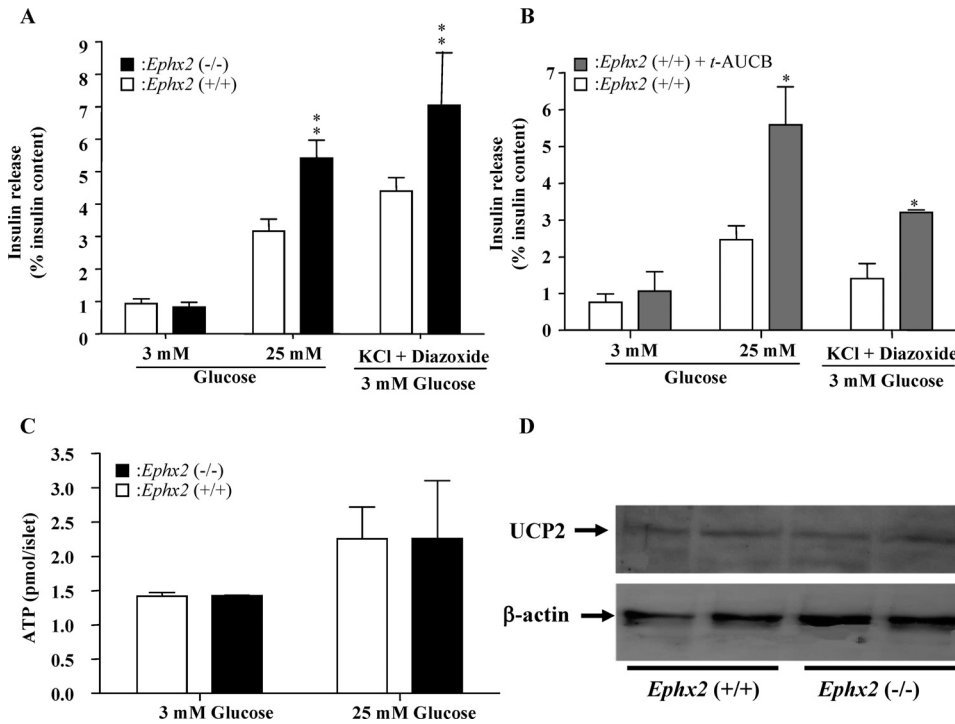
Fig. 6. GSIS, ATP levels, and UCP2 expression in $Ephx2(-/-)$ and $Ephx2(+/+)$ islets. A, $Epxh2(+/+)$ and $Epxh2(-/-)$ islets were treated with 3 mM glucose, 25 mM glucose, or 30 mM KCl plus 250 μM diazoxide plus 3 mM glucose. Insulin concentrations in the media and islet pellets were determined using an insulin ELISA kit. The data shown are based on the results of five experiments. B, islets were isolated from $Epxh2(+/+)$ mice incubated with either t-AUCB (100 μM) or vehicle for 12 h and then incubated with 3 mM glucose, 25 mM glucose, or 30 mM KCl plus 250 μM diazoxide plus 3 mM glucose. Insulin concentrations in the media and islet pellets were determined with an insulin ELISA kit. The data shown are based on the results of four experiments. C, ATP levels. After overnight culture, $Ephx2(-/-)$ or $Ephx2(+/+)$ islets were incubated with 3 or 25 mM glucose and then assessed for concentrations of ATP ($n = 3$). D, Western blot analysis of UCP2 in $Ephx2(-/-)$ and $Ephx2(+/+)$ islets. *, $P < 0.05$; **, $P < 0.01$ versus $Ephx2(+/+)$ incubated with vehicle.
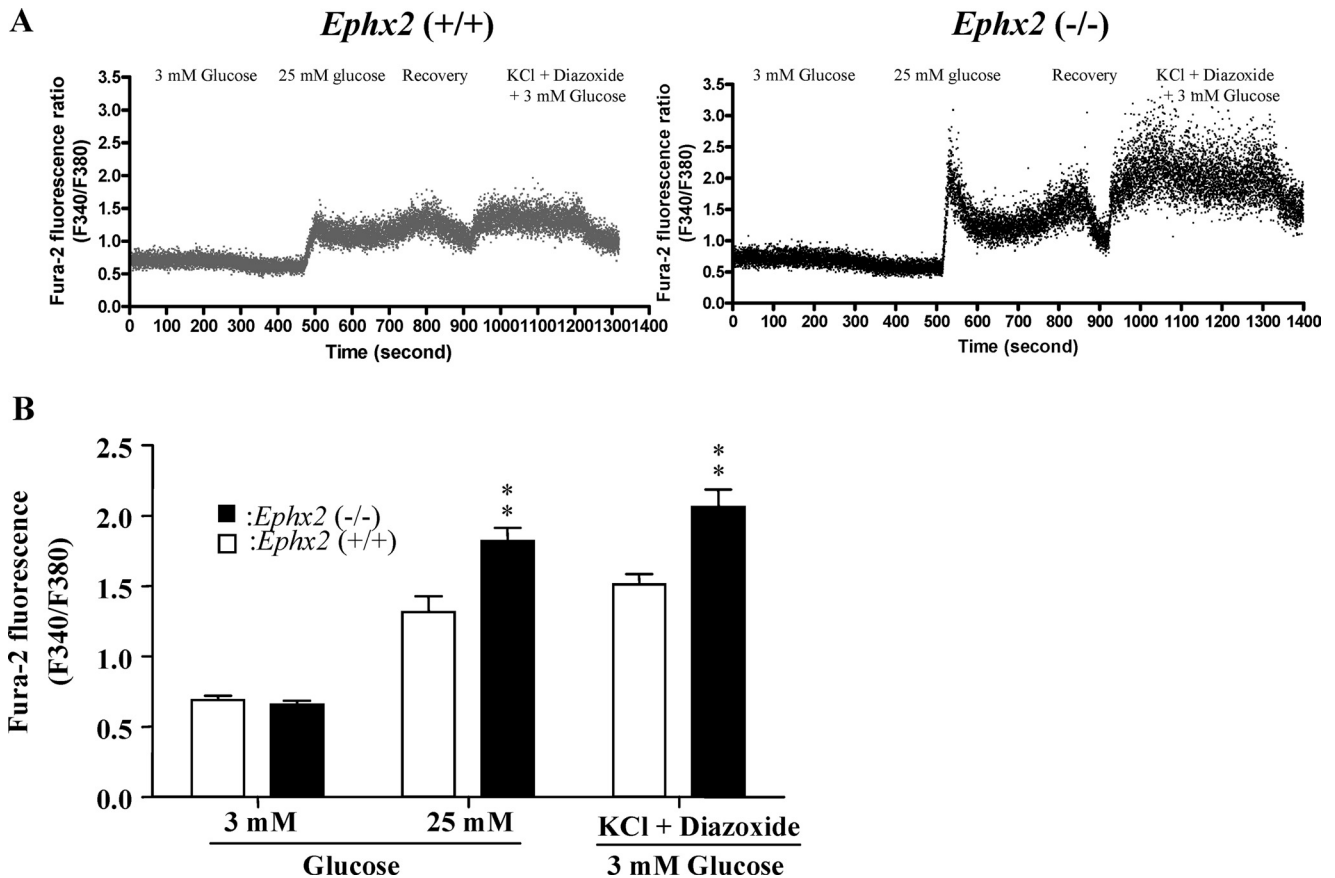

Fig. 7. Glucose-induced changes in $[Ca^{2+}]_i$ in $Ephx2(-/-)$ and $Ephx2(+/+)$ cells. A, representative Ca^{2+} traces obtained from individual $Ephx2(-/-)$ ($n = 19$) and $Ephx2(+/+)$ ($n = 16$) islet cells in response to 3 mM glucose, 25 mM glucose, or 30 mM KCl plus 250 μM diazoxide plus 3 mM glucose. B, quantitative summary of the $[Ca^{2+}]_i$ response to different stimulators. **, $P < 0.01$ versus $Ephx2(+/+)$ mice. Cells representing at least five different mice from each genotype were analyzed.

apoptosis and result in hyperglycemia. To determine whether sEH KO has any effects on apoptosis, 6-week-old male *Ephx2*(+/+) and *Ephx2*(−/−) mice were given either STZ (50 mg/kg/day for 3 days, i.p.) or vehicle. On day 14 after the initial STZ treatment, we examined islet cell apoptosis. As shown in Fig. 8A, we did not observe any apoptosis in pancreatic sections of *Ephx2*(+/+) or *Ephx2*(−/−) mice treated with vehicle. STZ treatment induced significant islet cell apoptosis in *Ephx2*(+/+) mice, but a marked reduction in islet cell apoptosis was observed in *Ephx2*(−/−) mice (Fig. 8).

Discussion

Because pancreatic β-cell loss and dysfunction are central factors in the pathogenesis of diabetes, preventing β-cell loss and diminishing β-cell dysfunction are potentially useful approaches to enhancing glucose homeostasis in diabetes (Henquin, 2004). Although it is well estab-

A

B

Fig. 8. A, in *Ephx2*(−/−) mice treated with vehicle, pancreases showed no apoptotic cell. In *Ephx2*(+/+) mice treated with vehicle, pancreases showed no apoptotic cell. On day 14 after STZ treatment, representative pancreatic photomicrography showed two apoptotic cells in islet of *Ephx2*(−/−) mice. On day 14 after STZ treatment, representative pancreatic photomicrography showed six apoptotic cells in islet of *Ephx2*(+/+) mice. B, quantification analysis of TUNEL assay showed that islet cell apoptosis in the STZ-*Ephx2*(+/+) group is significantly higher than in the STZ-*Ephx2*(−/−) group; $n = 4$. *, $P < 0.05$ versus STZ-*Ephx2*(+/+) mice.

lished that the inhibition of sEH lowers blood pressure in various animal models (Imig et al., 2002, 2005; Loch et al., 2007), the involvement of sEH in the control of blood glucose in diabetes is unknown. Here, for the first time, we show that sEH has a role in glucose homeostasis, insulin secretion, and islet cell apoptosis.

Because insulin is the major hormone that lowers blood glucose levels, we hypothesized that sEH has a critical function in regulating insulin homeostasis and examined the effect of sEH KO on glucose homeostasis in STZ mice. Glucose tolerance tests of STZ mice showed that sEH KO improved glucose tolerance and increased plasma insulin concentrations (Fig. 3, A and B). These results suggest that preventing hyperglycemia by sEH KO in diabetic mice is probably the result of increased GSIS in pancreatic β cells. To test this possibility, we did hyperglycemic clamp study of *Ephx2*(−/−) and *Ephx2*(+/+) mice, finding that sEH KO significantly enhanced insulin secretion (Fig. 4C). Because insulin sensitivity is equal in *Ephx2*(+/+) and *Ephx2*(−/−) mice (Fig. 5A), these results show that *Ephx2*(−/−) mice release more insulin than do *Ephx2*(+/+) mice without changing their insulin sensitivity.

Insulin is secreted by pancreatic β cells in response to high glucose, whereas glucagon is secreted by pancreatic α cells during hypoglycemia. Under normal physiological conditions, elevated glucose or insulin levels inhibit glucagon release from α cells (Gromada et al., 2009). Insulin promotes glucose uptake from peripheral tissues and stimulates the synthesis of glycogen and lipids, whereas glucagon opposes the actions of insulin (Gromada et al., 2009). Thus, the balance between these two hormones holds blood glucose levels within a narrow physiological range. To determine whether sEH KO affects circulating levels of glucagon, we measured fed and fasted plasma glucagon concentrations in *Ephx2*(−/−) and *Ephx2*(+/+) mice. We found that these mice had comparable levels of plasma glucagon (Fig. 5B), indicating that the effects of sEH KO on glucose homeostasis are caused by insulin rather than glucagon.

Because sEH KO promotes insulin secretion in vivo, we determined whether sEH is significantly expressed in islets and β cells. Using purified sEH, we estimated that the concentration of sEH in mouse islets is approximately 0.93 ng/μg protein (Fig. 1C). Thus, a significant amount of sEH is expressed in islets. To determine whether sEH is expressed in β cells, we used an immunohistochemical method in an attempt to determine the expression of sEH in pancreatic cells. We tried two sources of antibodies: Dr. B. D. Hammock and Santa Cruz Biotechnology, Inc. (Santa Cruz, CA). However, these antibodies were not suitable for immunohistochemical analysis (data not shown). Alternatively, we did Western blot analysis of sEH in NIT-1 cells (nonobese diabetic-derived β-cell line), finding that sEH is expressed in NIT-1 cells (Fig. 1D). This suggests that sEH is expressed in β cells.

To investigate the mechanism for the stimulation of insulin release by sEH KO in glucose homeostasis, we assessed whether sEH KO and inhibition affect islet GSIS. We found that both sEH KO and inhibition significantly stimulated islet GSIS, suggesting that deletion and inhibition of sEH are involved in enhancing GSIS in pancreatic β cells. It is well established that the K_{ATP} channel-dependent pathway is essential in the stimulation of insu-
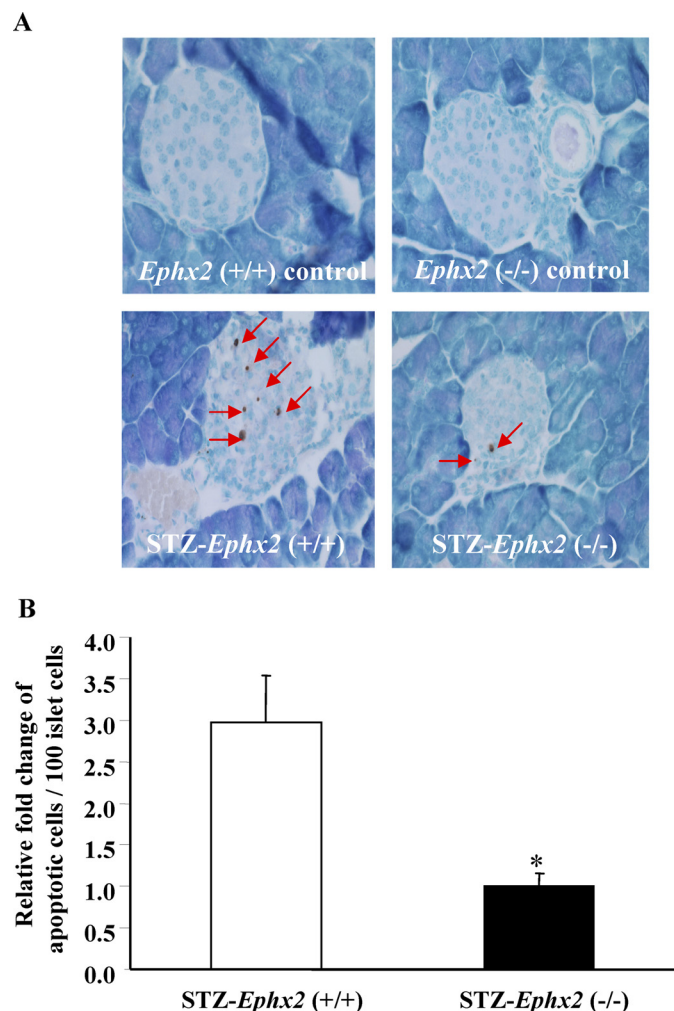
lin secretion by glucose and has the vital function of triggering the pathway for GSIS in β cells (Chan et al., 2004; Gupta et al., 2005; Henquin, 2009). In the K_{ATP} channel-dependent pathway for insulin release, it occurs as follows: glucose is oxidized in β cells to generate NADH and $FADH_2$, which donate electrons to the electron transport chain located in the mitochondrial matrix to create a proton electrochemical gradient; protons then re-enter the mitochondrial matrix to generate ATP; increased ATP closes the K_{ATP} channel, causing membrane depolarization, increasing the cytoplasmic calcium concentration, and consequently activating insulin secretion through calcium-dependent exocytosis (Zhang et al., 2001; Gupta et al., 2005; Kahn et al., 2006). Because ATP and UCP2 are the key components of this pathway, we next determined whether sEH KO affects ATP content and UCP2 levels in islets. We found no difference between $Ephx2(-/-)$ and $Ephx2(+/+)$ islets with response to ATP content (Fig. 6C) or UCP2 expression (Fig. 6D), suggesting that the mechanism that stimulates insulin release by sEH KO probably is not mediated through the K_{ATP} channel-dependent pathway.

It is widely accepted that any pharmacological agents interfering with elevation of $[Ca^{2+}]_i$ in β cells causes impairment of GSIS, whereas any agents that increase $[Ca^{2+}]_i$ promote insulin release in β cells (Henquin, 2009). Thus, $[Ca^{2+}]_i$ serves as a triggering signal for insulin release in β cells (Henquin, 2000). To examine whether sEH KO affects $[Ca^{2+}]_i$ in response to different stimulators, we did calcium photometry analysis in cultured $Ephx2(-/-)$ and $Ephx2(+/+)$ islet cells. We found that $[Ca^{2+}]_i$ increased more rapidly in $Ephx2(-/-)$ islet cells than it did in $Ephx2(+/+)$ islet cells in response to both high glucose and high KCl plus diazoxide, an approach used to evaluate the amplifying pathway (Henquin, 2000) (Fig. 7). These findings indicate that the effects of sEH KO on the enhancement of islet GSIS are mediated through the amplifying pathway. However, the molecular mechanisms whereby sEH KO enhances islet GSIS through this pathway require further investigation.

The present study provides new information about the prevention of hyperglycemia by sEH KO and inhibition in diabetes, as well as the beneficial effect of sEH KO and inhibition on islet GSIS. Nevertheless, the exact mechanisms by which sEH KO or inhibition prevents hyperglycemia and influences insulin secretion are still not known.

The possible reasons for the effects of sEH KO or inhibition in vitro and in vivo may be explained as follows. Although the promotion of islet GSIS by sEH KO is an important reason for the prevention of hyperglycemia in STZ mice, other biological activity derived from sEH KO can contribute to this beneficial effect. Abundant evidence indicates that immune cell–secreted proinflammatory cytokines are important in the pathogenesis of STZ-induced diabetes (Müller et al., 2002; Fukuda et al., 2008). Because proinflammatory cytokines are also important in the causation of β-cell apoptosis, we hypothesize that the prevention of hyperglycemia by sEH KO is the result of its antiapoptotic property. To test this hypothesis, we determined whether sEH KO affects islet cell apoptosis in an STZ model, finding that STZ-$Ephx2(-/-)$ mice exhibited lower islet cell apoptosis than did STZ-$Ephx2(+/+)$ mice (Fig. 8). Simpkin et al. (2009) have recently shown that the inhibition of sEH by 12-(3-adamantane-1-yl-ureido)dodecanoic acid decreases the expression of proapoptotic genes in neural tissues. Taken together, these results show that the antiapoptotic property of sEH KO in islets is an important mechanism in preventing hyperglycemia in diabetes.

It is well accepted that sEH KO and inhibition increase EET levels by decreasing the degradation of EETs (Chiamvimonvat et al., 2007). In accord with this, Liu et al. (2009) have shown that t-AUCB treatment reduces the production of DHETs and increases the ratios of EETs to DHETs in the plasma of lipopolysaccharide-treated mice. Likewise, Seubert et al. (2006) reported that $Ephx2(-/-)$ mice have higher plasma ratios of EETs to DHETs than do wild-type mice. Thus, it is likely that sEH KO or inhibition by t-AUCB causes elevation of pancreatic EET levels and contributes to the enhancement of GSIS. In this regard, Zeldin et al. (1997) reported that CYP2J protein is expressed in human and rat pancreatic tissues and noted that significant amounts of endogenous EETs are present in the human and rat pancreas. Falck et al. (1983) have shown that EETs are potent mediators of insulin release in isolated rat islets. Nevertheless, it remains unclear which P450 isoforms are responsible for the generation of EETs in the mouse pancreas and whether EETs are able to promote insulin release in mouse islets.

In summary, we have made the novel findings that sEH KO and inhibition prevent hyperglycemia of STZ-diabetic mice. Our hyperglycemic clamp experiments support the possibility that the prevention of hyperglycemia by sEH KO is caused by increased insulin secretion from β cells. Our in vitro findings show that sEH KO and its inhibition increase GSIS by islets. It appears that the enhancement of GSIS by sEH KO in β cells is mediated through the amplifying pathway, and sEH KO reduces islet apoptosis during diabetes. Because both sEH KO and sEH inhibitor prevent the elevation of blood glucose levels in diabetic animals, this study raises the possibility that, in addition to their antihypertensive and anti-inflammatory effects, sEH KO and inhibitors may be promising approaches to the prevention of hyperglycemia in diabetes mellitus.

References

Breyer MD, Böttinger E, Brosius FC 3rd, Coffman TM, Harris RC, Heilig CW, Sharma K, and AMDCC (2005) Mouse models of diabetic nephropathy. *J Am Soc Nephrol* **16:**27–45.
Chan CB, Saleh MC, Koshkin V, and Wheeler MB (2004) Uncoupling protein 2 and islet function. *Diabetes* **53:**S136–S142.
Chiamvimonvat N, Ho CM, Tsai HJ, and Hammock BD (2007) The soluble epoxide hydrolase as a pharmaceutical target for hypertension. *J Cardiovasc Pharmacol* **50:**225–237.
Dai T, Patel-Chamberlin M, Natarajan R, Todorov I, Ma J, LaPage J, Phillips L, Nast CC, Becerra D, Chuang P, et al. (2009) Heat shock protein 27 overexpression mitigates cytokine-induced islet apoptosis and streptozotocin-induced diabetes. *Endocrinology* **150:**3031–3039.
Danial NN, Walensky LD, Zhang CY, Choi CS, Fisher JK, Molina AJ, Datta SR, Pitter KL, Bird GH, Wikstrom JD, et al. (2008) Dual role of proapoptotic BAD in insulin secretion and beta cell survival. *Nat Med* **14:**144–153.
Deng Y, Theken KN, and Lee CR (2010) Cytochrome P450 epoxygenases, soluble

epoxide hydrolase, and the regulation of cardiovascular inflammation. *J Mol Cell Cardiol* **48:**331–341.

Donath MY, Størling J, Berchtold LA, Billestrup N, and Mandrup-Poulsen T (2008) Cytokines and beta-cell biology: from concept to clinical translation. *Endocr Rev* **29:**334–350.

Falck JR, Manna S, Moltz J, Chacos N, and Capdevila J (1983) Epoxyeicosatrienoic acids stimulate glucagon and insulin release from isolated rat pancreatic islets. *Biochem Biophys Res Commun* **114:**743–749.

Fukuda K, Tesch GH, Yap FY, Forbes JM, Flavell RA, Davis RJ, and Nikolic-Paterson DJ (2008) MKK3 signalling plays an essential role in leukocyte-mediated pancreatic injury in the multiple low-dose streptozotocin model. *Lab Invest* **88:**398–407.

Gembal M, Gilon P, and Henquin JC (1992) Evidence that glucose can control insulin release independently from its action on ATP-sensitive K^+ channels in mouse B cells. *J Clin Invest* **89:**1288–1295.

Gromada J, Duttaroy A, and Rorsman P (2009) The insulin receptor talks to glucagon? *Cell Metab* **9:**303–305.

Gupta RK, Vatamaniuk MZ, Lee CS, Flaschen RC, Fulmer JT, Matschinsky FM, Duncan SA, and Kaestner KH (2005) The MODY1 gene HNF-4alpha regulates selected genes involved in insulin secretion. *J Clin Invest* **115:**1006–1015.

Henquin JC (2000) Triggering and amplifying pathways of regulation of insulin secretion by glucose. *Diabetes* **49:**1751–1760.

Henquin JC (2004) Pathways in beta-cell stimulus-secretion coupling as targets for therapeutic insulin secretagogues. *Diabetes* **53:**S48–S58.

Henquin JC (2009) Regulation of insulin secretion: a matter of phase control and amplitude modulation. *Diabetologia* **52:**739–751.

Imig JD (2005) Epoxide hydrolase and epoxygenase metabolites as therapeutic targets for renal diseases. *Am J Physiol Renal Physiol* **289:**F496–F503.

Imig JD (2006) Cardiovascular therapeutic aspects of soluble epoxide hydrolase inhibitors. *Cardiovasc Drug Rev* **24:**169–188.

Imig JD, Zhao X, Capdevila JH, Morisseau C, and Hammock BD (2002) Soluble epoxide hydrolase inhibition lowers arterial blood pressure in angiotensin II hypertension. *Hypertension* **39:**690–694.

Inscho EW, LeBlanc EA, Pham BT, White SM, and Imig JD (1999) Purinoceptor-mediated calcium signaling in preglomerular smooth muscle cells. *Hypertension* **33:**195–200.

Institute of Laboratory Animal Resources (1996) *Guide for the Care and Use of Laboratory Animals*, 7th ed, Institute of Laboratory Animal Resources, Commission on Life Sciences, National Research Council, Washington, DC.

Kahn SE, Hull RL, and Utzschneider KM (2006) Mechanisms linking obesity to insulin resistance and type 2 diabetes. *Nature* **444:**840–846.

Krauss S, Zhang CY, Scorrano L, Dalgaard LT, St-Pierre J, Grey ST, and Lowell BB (2003) Superoxide-mediated activation of uncoupling protein 2 causes pancreatic beta cell dysfunction. *J Clin Invest* **112:**1831–1842.

Liu JY, Tsai HJ, Hwang SH, Jones PD, Morisseau C, and Hammock BD (2009) Pharmacokinetic optimization of four soluble epoxide hydrolase inhibitors for use in a murine model of inflammation. *Br J Pharmacol* **156:**284–296.

Loch D, Hoey A, Morisseau C, Hammock BO, and Brown L (2007) Prevention of hypertension in DOCA-salt rats by an inhibitor of soluble epoxide hydrolase. *Cell Biochem Biophys* **47:**87–98.

Mazzone T (2009) Hyperglycaemia and coronary heart disease: the meta picture. *Lancet* **373:**1737–1738.

Müller A, Schott-Ohly P, Dohle C, and Gleichmann H (2002) Differential regulation of Th1-type and Th2-type cytokine profiles in pancreatic islets of C57BL/6 and BALB/c mice by multiple low doses of streptozotocin. *Immunobiology* **205:**35–50.

Oshima H, Taketo MM, and Oshima M (2006) Destruction of pancreatic beta-cells by transgenic induction of prostaglandin E2 in the islets. *J Biol Chem* **281:**29330–29336.

Roman RJ (2002) P-450 metabolites of arachidonic acid in the control of cardiovascular function. *Physiol Rev* **82:**131–185.

Seubert JM, Sinal CJ, Graves J, DeGraff LM, Bradbury JA, Lee CR, Goralski K, Carey MA, Luria A, Newman JW, et al. (2006) Role of soluble epoxide hydrolase in postischemic recovery of heart contractile function. *Circ Res* **99:**442–450.

Simpkins AN, Rudic RD, Schreihofer DA, Roy S, Manhiani M, Tsai HJ, Hammock BD, and Imig JD (2009) Soluble epoxide inhibition is protective against cerebral ischemia via vascular and neural protection. *Am J Pathol* **174:**2086–2095.

Sinal CJ, Miyata M, Tohkin M, Nagata K, Bend JR, and Gonzalez FJ (2000) Targeted disruption of soluble epoxide hydrolase reveals a role in blood pressure regulation. *J Biol Chem* **275:**40504–40510.

Uysal KT, Wiesbrock SM, Marino MW, and Hotamisligil GS (1997) Protection from obesity-induced insulin resistance in mice lacking TNF-alpha function. *Nature* **389:**610–614.

Yoon JC, Puigserver P, Chen G, Donovan J, Wu Z, Rhee J, Adelmant G, Stafford J, Kahn CR, Granner DK, et al. (2001) Control of hepatic gluconeogenesis through the transcriptional coactivator PGC-1. *Nature* **413:**131–138.

Zeldin DC, Foley J, Boyle JE, Moomaw CR, Tomer KB, Parker C, Steenbergen C, and Wu S (1997) Predominant expression of an arachidonate epoxygenase in islets of Langerhans cells in human and rat pancreas. *Endocrinol*ogy **138:**1338–1346.

Zhang CY, Baffy G, Perret P, Krauss S, Peroni O, Grujic D, Hagen T, Vidal-Puig AJ, Boss O, Kim YB, et al. (2001) Uncoupling protein-2 negatively regulates insulin secretion and is a major link between obesity, beta cell dysfunction, and type 2 diabetes. *Cell* **105:**745–755.

Address correspondence to: Mong-Heng Wang, Department of Physiology, Medical College of Georgia, Augusta, GA 30912. E-mail: mwang@mail.mcg.edu